Long-term study of medium-scale traveling ionospheric disturbances using O I 630 nm all-sky imaging and ionosonde over Brazilian low latitudes

D. C. M. Amorim,[1] A. A. Pimenta,[1] J. A. Bittencourt,[1] and P. R. Fagundes[2]

[1] In this paper, we report a long-term study of medium-scale traveling ionospheric disturbance (MSTID) occurrence using all-sky images of O I 630 nm airglow emission. Our study is based on a 10.5 year data series in which 5.5 years compound a new data set. The images were obtained by an all-sky imager installed at Cachoeira Paulista (22.7°S, 45°W, 15°S magnetic latitude). Our results show the greatest occurrence of MSTIDs during solar minimum and a minor occurrence rate during descending and ascending solar activity periods. During solar maximum, we have not detected MSTID signatures on all-sky images. All detected events have occurred during geomagnetically quiet conditions. Simultaneous measurements using both all-sky images and ionograms obtained at the same site show the occurrence of spread F and a sharp rise in the ionospheric F layer at the same time as dark bands are optically registered over the zenith. It is possible that for certain weaker events, the ionosonde may resolve bands that are not sufficiently raised to cause darkening of the all-sky images. In order to investigate this possibility, we have conducted a study using only ionograms for a 1 year period (March 2000–February 2001) during solar maximum, when we have not seen any MSTID events in the all-sky images. As we conjectured, MSTIDs also occur during solar maximum, and the risings of the ionospheric F layer are not able to disturb the airglow layer during such events.

1. Introduction

[2] Medium-scale traveling ionospheric disturbances (MSTIDs), probably related to midlatitude electrodynamics instability processes, have been observed over low latitudes in the Brazilian sector, using all-sky images of the O I 630 nm nightglow emission. A wide-angle optical imaging system is installed at Cachoeira Paulista (22.7°S, 45°W, 15°S magnetic latitude (MLAT)), Brazil. MSTIDs are seen like dark band structures that propagate from southeast to northwest with an average speed of 50–200 m/s at an altitude range of 220–300 km [*Pimenta et al.*, 2008a, 2008b; *Candido et al.*, 2008]. The dark band pattern refers to depletions in the O I 630 nm airglow emission due to vertical movements of the *F* layer. Since the O I 630 nm emission intensity is strongly dependent on the electronic concentration, its tendency is to decrease or increase as the *F* layer plasma moves upward or downward.

[3] *Pimenta et al.* [2008b] presented a statistical study of the occurrence of MSTIDs, over the Brazilian sector, based on a 5 year data set, regarding on high, low and ascending solar activity periods. They have observed a maximum occurrence rate during the solar minimum and no occurrences were detected during the solar maximum. *Candido et al.* [2008], based on the analysis of 28 events along 7 years, also observed an inverse dependence of the occurrence of MSTIDs with the solar cycle, over Cachoeira Paulista, and reported a seasonal behavior of the occurrence of MSTIDs, with a peak during the local winter.

[4] In the Japanese sector, *Shiokawa et al.* [2003] reported a statistical analysis of the occurrence of MSTIDs for the period from October 1998 to September 2000. It shows most of occurrences during solstice months, where the major peak occurs during the summer solstice. In Arecibo, *Garcia et al.* [2000] presented a statistical analysis regarding the period from January 1997 to March 1998, which shows most of occurrences of MSTIDs during the local winter. A recent study based on the analysis of 942 nights between 2002 and 2007 shows a semiannual pattern with peak of occurrence at both solstices in Arecibo [*Martinis et al.*, 2010].

[5] In this work we present the results obtained by an extensive study using both airglow images and ionosonde

[1]Instituto Nacional de Pesquisas Espaciais, Sao Jose dos Campos, Brazil.
[2]Physics and Astronomy, Universidade do Vale do Paraiba, Sao Jose dos Campos, Brazil.

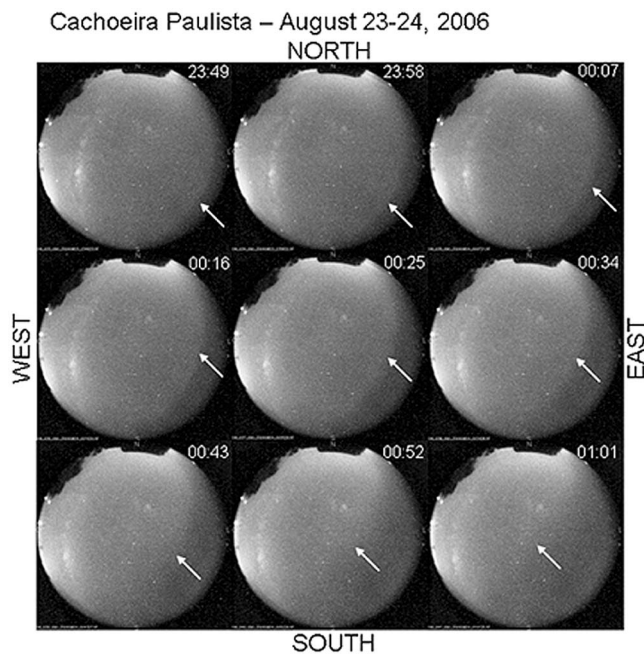Cachoeira Paulista – August 23-24, 2006

NORTH

Figure 1. All-sky images of the O I 630 nm airglow emission obtained on 23–24 August 2006. In this example, the dark band structure, indicated by the white arrow, entered from southeast and moved across the field of view toward the northwest at an altitude range of 220–300 km.

data. In order to verify the MSTID behavior, we have made three different data analyses. In the first one, we analyzed 10.5 years of airglow images, in which 5.5 among them compound a new data set. This large data set has permitted us to investigate the MSTIDs' behavior compared with solar activity conditions and seasonality. The second analysis is based on the simultaneous analysis using data from both airglow images and ionograms, which has permitted us to investigate the changes in ionospheric F layer density profile during MSTID events. Finally, based in the results obtained in the second analysis, we could make a third one based only on ionosonde data during solar maximum, in order to investigate the occurrence of MSTIDs during this phase of the solar cycle, since all-sky imager have not detected any signature of this phenomenon in the airglow layer.

2. Measurement Techniques and Observations

[6] The all-sky images that we have used were obtained from an all-sky imaging system installed at Cachoeira Paulista (22.7°S, 45°W, 15°S MLAT). The all-sky imaging system can measure airglow emissions in several spectral lines through the use of optical interference filters. The instrument detects spatial and temporal variations of the intensity of airglow emission layers. In our study we have used the O I 630 nm emission which the emission layer is located at approximately 220–300 km height.

[7] We have used images for the periods from January 1990 to December 1990 (high solar activity period, average $F_{10.7}$ cm flux > 180 × 10^{-22} Wm^{-2} Hz^{-1}), May 1995 to July 1996 (low solar activity period, average $F_{10.7}$ cm flux < 70 × 10^{-22} Hz^{-1}), January 1997 to December 2000 (ascending solar activity period, average $F_{10.7}$ cm flux

from 70 × 10^{-22} Wm^{-2} Hz^{-1} to 170 × 10^{-22} Wm^{-2} Hz^{-1}), July 2004 to December 2007 (descending solar activity period, average $F_{10.7}$ cm flux from 90 × 10^{-22} Wm^{-2} Hz^{-1} to 160 × 10^{-22} Wm^{-2}) and from January 2008 to December 2008 (low solar activity period, average $F_{10.7}$ cm flux < 70 × 10^{-22} Wm^{-2} Hz^{-1}). We have observed an amount of 4576 h, of which 503 h showed the occurrence of MSTIDs.

[8] For the period between 1990 and 2000 we have used O I 630 nm nightglow emission images obtained from an imager that uses a conventional single lens reflex camera. This imager was operational at Cachoeira Paulista from 1987 to 2000. The images are monochromatic and were recorded on 35 mm films. For the period 2004 to 2008 we used digital images obtained from an all-sky imager with a CCD camera. The latter has higher resolution than the former. For more details about the instruments, see *Pimenta et al.* [2001] and *Garcia et al.* [1997].

[9] The O I 630 nm nightglow emission is generated by dissociative recombination of the molecular ion O_2^+. This generation mechanism involves two steps. The first step ($O^+ + O_2 \rightarrow O_2^+ + O$) is the process of ionization of molecular oxygen O_2 by a charge exchange reaction. The second step ($O_2^+ + e \rightarrow O + O*(^1D)$) is the mechanism of dissociative recombination of O_2^+ that results in an excited oxygen atom at the ^1D level. When decaying spontaneously to the ground state (^3P), the excess of energy is converted on photon radiation at the wavelength 630 nm. The emission intensity depends on the O_2^+ and electron concentration. Therefore, it is strongly dependent on the vertical motions of the ionospheric plasma, in such a way that, when the ionospheric layer moves upward, the intensity decreases, and when it moves downward, the intensity is enhanced.

[10] Figure 1 shows a sequence of raw all-sky images in the O I 630 nm emission obtained on 23–24 August 2006, from 23:49 to 01:01 LT, for a geomagnetically quiet night (Kp < 3). From Figure 1 (top middle), we can see a dark band structure, indicated by white arrows, which comes
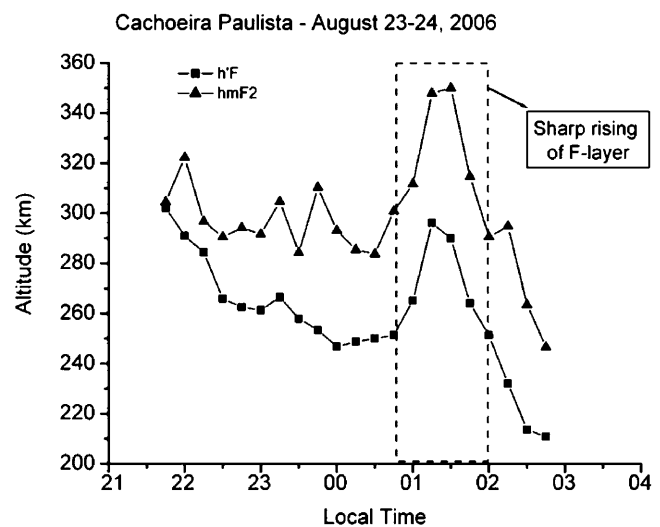

Figure 2. Temporal variation of the ionospheric parameters $h'F$ and h_mF_2 for the night of 23–24 August 2006. The dashed rectangle emphasizes the abrupt rise of the F layer around 01:00 LT.
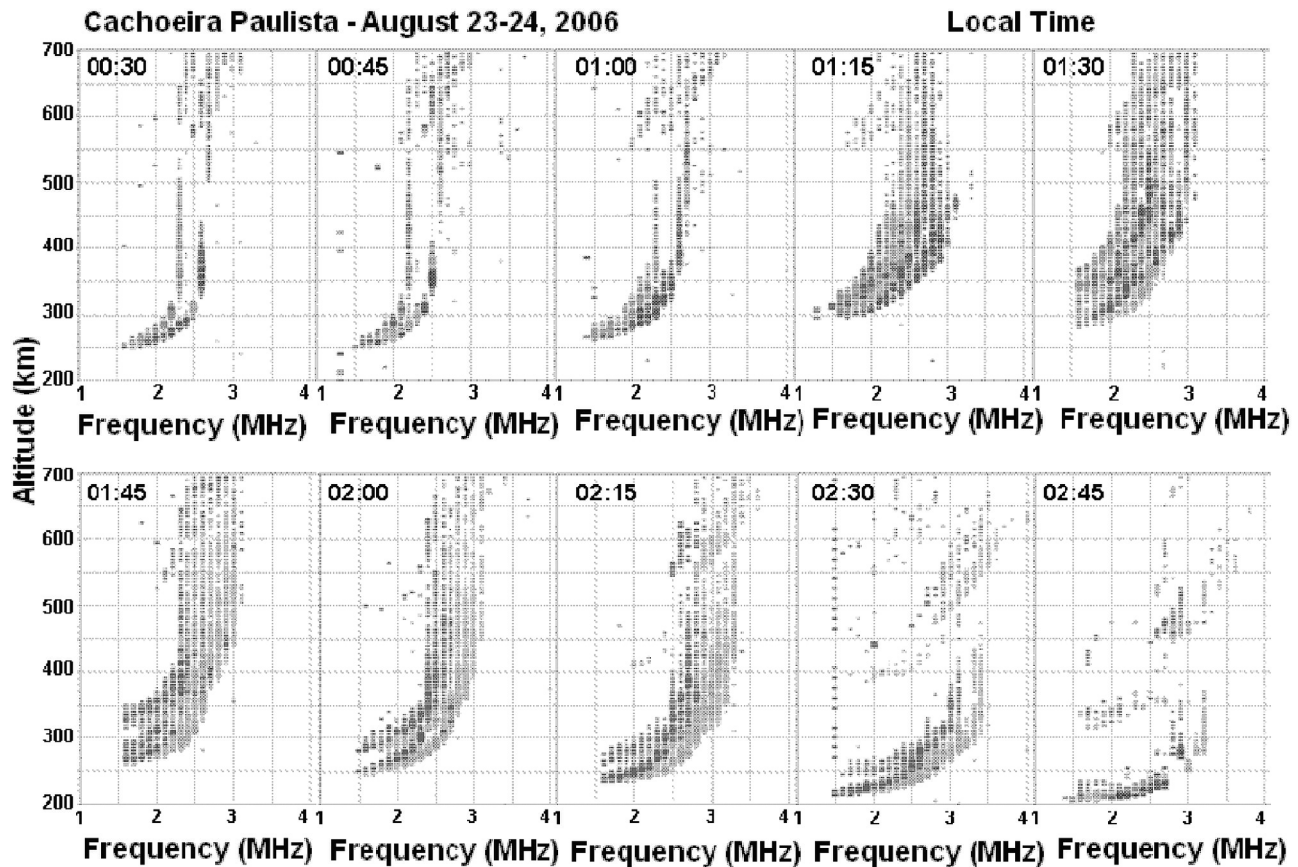
Figure 3. Ionograms obtained on 23–24 August 2006 with the digisonde installed at Cachoeira Paulista. This sequence shows the occurrence of spread F at the same time as the all-sky images registered MSTIDs over the zenith of Cachoeira Paulista and ionospheric parameters registered abrupt uplifting of both the peak height and virtual height of the ionospheric F layer.

from southeast and crosses the imager field of view, propagating toward northwest, reaching the zenith around 01:00 LT (04:00 UT).

[11] A digisonde DGS 256, installed at the same site was used to provide ionospheric F layer parameters through vertical sounding. Details about the instrument can be found in the work of *Reinisch et al.* [1989]. Figure 2 shows a plot of the temporal variation of ionospheric parameters $h'F$ and h_mF_2, and refers to the same date as the sequence of images in Figure 1. The Digisonde observations registered abrupt increases in both the F layer peak height (h_mF_2) and F layer bottomside virtual height ($h'F$) on 23–24 August 2006, when the low-intensity band passed over Cachoeira Paulista. From simultaneous analysis we can see that the dark band structure observed in the all-sky images corresponds to zones of depleted airglow due to the uplift of ionospheric F layer. Ionosonde data also registered the occurrence of spread F associated with the events, as illustrated in Figure 3. It is important to be pointed out that we have analyzed data for all geomagnetic conditions, but MSTID cases were only found during geomagnetically quiet nights.

3. Data Analysis

[12] Our work is based on three types of analysis using all-sky images and ionograms. The results obtained in the first analysis show some features common to all events. These features are the preferential alignment (southwest-northeast) and propagation (northwestward) directions of the dark bands and the occurrence limited to geomagnetically quiet nights (Kp < 3).

[13] The second analysis was done by comparing simultaneous data from both all-sky images and ionograms. The results obtained show sharp rises of the F layer and the occurrence of spread F during MSTID events.

[14] The third one is an additional study based on the analysis of ionograms for the period of solar maximum. It was made in order to investigate the possible occurrence of MSTIDs during this phase of the solar cycle. On the basis of our ionosonde observations, raised MSTID-like bands are present during solar maximum, but they are not raised sufficiently to darken the all-sky images.

3.1. All-Sky Image Analysis

[15] Using a computational routine in IDL environment, it was possible to linearize the all-sky images and to calculate parameters like phase velocity and azimuthal angle of the dark bands. The linearizing process is important in order to remove effects of compression and curving imposed by the all-sky lens [*Garcia et al.*, 1997]. The images were linearized in such a way that one pixel corresponds to 1 km,
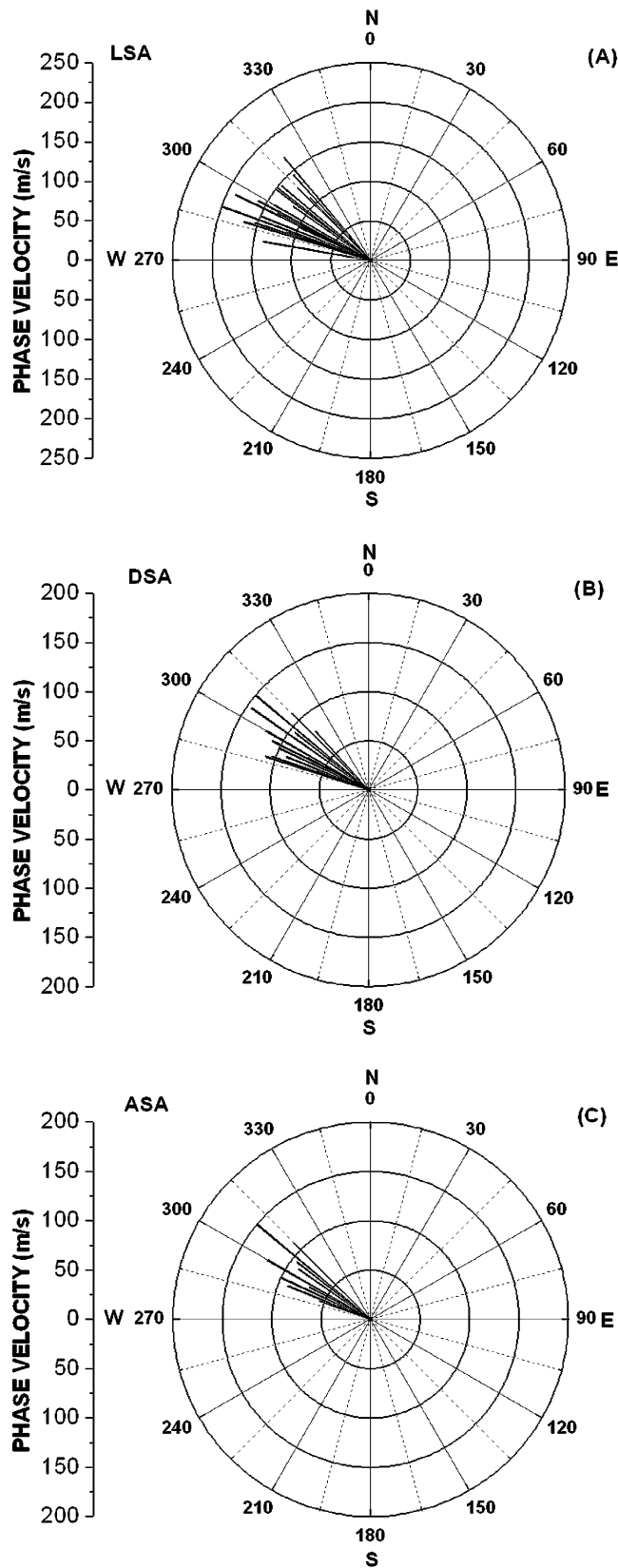
on a grid of 1024×1024 km^2. During solar minimum, the average velocity of MSTIDs was computed as being around 150 m/s. During descending and ascending solar activity periods the average velocity is around 100 m/s. Azimuthal distribution is highly anisotropic in all cases, exhibiting preferred directions northwestward with azimuths of 280°–320°. These parameters are graphically represented in Figure 4, in which the distribution of speeds is plotted in a 50 m/s interval. The length of each line indicates the phase velocity of MSTIDs detected during low, descending and ascending solar activity periods. Figures 4a and 4b are results obtained in a previous work [*Pimenta et al.*, 2008b] and were used here for comparison with our new result shown in Figure 4c. A detailed description of the linearization process can be found in the work of *Garcia et al.* [1997].

[16] We have observed 4576 h of clear sky during 10.5 years as shown in Figure 5. Gray bars refers to the period of optical observation (hours) and the dark gray bars refers to the MSTID occurrence rate (%). It is clearly seen that the occurrence rate is anticorrelated to the solar cycle.

[17] Figure 6 shows the nocturnal variation of the MSTID occurrence, which also changes with the solar cycle. During solar minimum, the period of occurrence is between 21:00 LT and 05:00 LT, and the maximum occurrence is around 01:30 LT. During descending and ascending solar activity periods, the occurrence is between 21:00 LT and 03:00 LT, and the maximum occurrence is around 23:30 LT and 24:30 LT. Thus, the lifetime of MSTIDs is higher during solar minimum, where the period of occurrence is almost 2 h larger than in the other phases of the solar cycle. Figure 7 depicts the seasonal occurrence of MSTIDs which shows a peak during winter time.

3.2. Comparisons Between Both Airglow Images and Ionograms

[18] As mentioned before, the O I 630 nm emission intensity is strongly dependent on the vertical movements of the ionospheric plasma during the night. Since the O I 630 nm airglow emission peak is situated at an altitude around 250 km, it is possible to analyze vertical movements
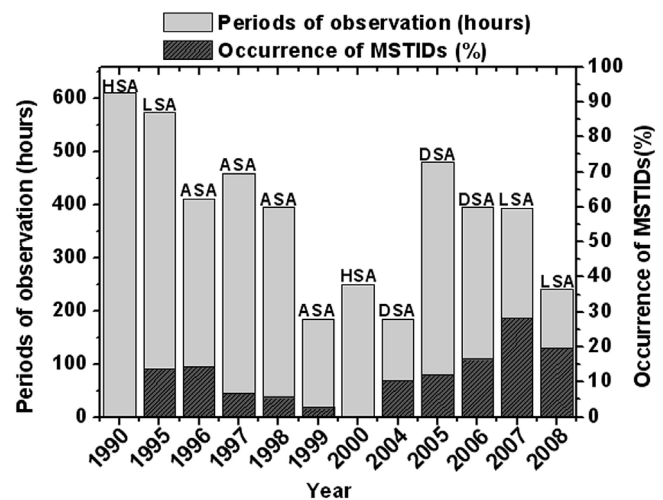
Figure 4. Nighttime azimuthal distribution and velocity of MSTIDs observed by all-sky images during (a) low solar activity period (LSA), (b) descending solar activity period (DSA), and (c) ascending solar activity period (ASA).

Figure 5. Occurrence of MSTIDs as a function of solar cycle. HSA refers to high solar activity period.
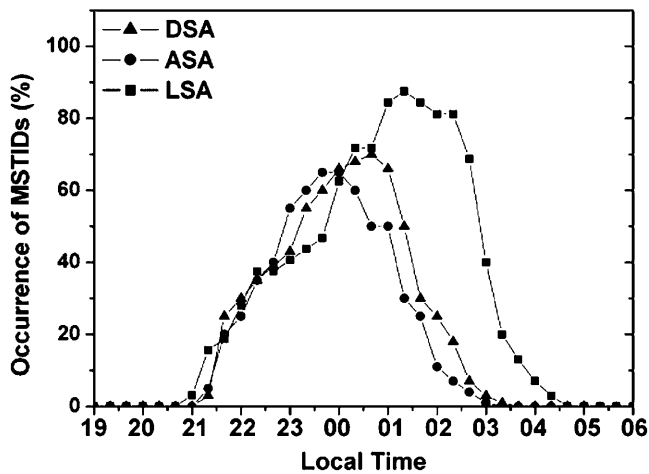
Figure 6. Nocturnal variation of the occurrence of MSTIDs during LSA, ASA, and DSA.

of the F layer plasma through the ionospheric parameters $h'F$ (F layer bottomside virtual height) and h_mF_2 (F layer peak height), provided by ionosonde measurements. As shown in Figure 2, the temporal variation of the ionospheric parameters reveals a sharp rising of the ionospheric F layer.

[19] For all the cases that we have simultaneous data from both all-sky images and ionograms, we have observed the occurrence of spread F at the same time as the dark bands passes over the zenith of Cachoeira Paulista. However, since we do not have simultaneous data for all cases studied, it is not possible to assert the correlation between MSTIDs and spread F. Shiokawa et al. [2003] in a simultaneous analysis of all-sky images and ionograms for two observation sites in the Japanese sector have found only 10% and 15% of spread F for the intervals when the MSTID structures were seen in the airglow images.
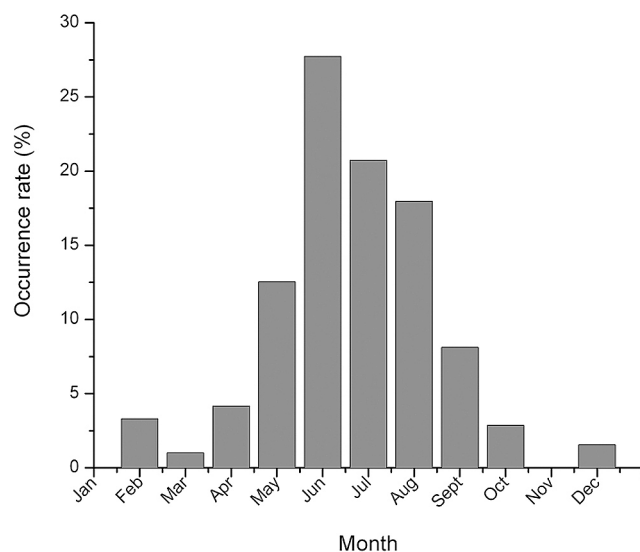

Figure 7. Seasonal variation of the occurrence of MSTIDs over the Brazilian sector.
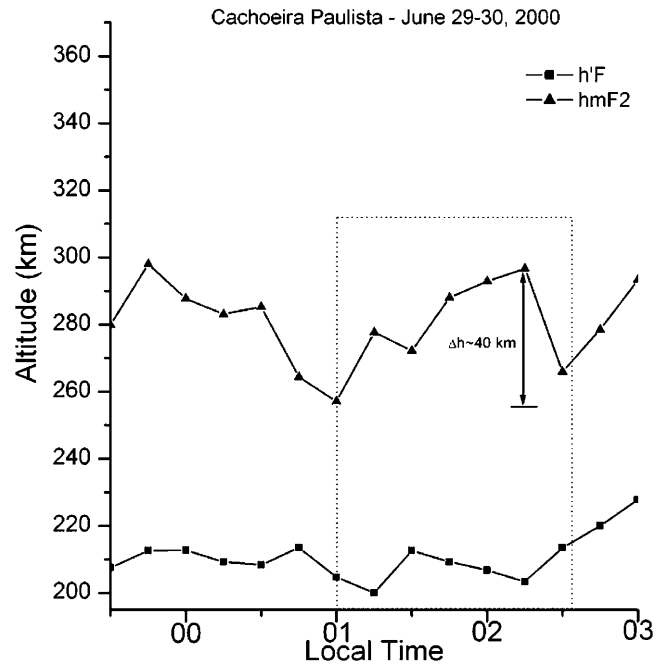

Figure 8. Temporal variation of the ionospheric parameters $h'F$ and h_mF_2 for the night of 29–30 June 2000. The dashed rectangle emphasizes the rise of the F layer around 02:00 LT.

3.3. Investigation of the Occurrence of MSTIDs During Solar Maximum

[20] The lack of the airglow observations during solar maximum does not necessarily mean that MSTIDs are not present. It is possible that raised bands can be detected by ionosondes, which are not sufficient to register in the airglow. In order to check this possibility, we have made a study based only on ionosonde data, examining the ionospheric parameters $h'F$ and h_mF_2. We have considered features like the occurrence of risings of the F layer, spread F in the ionograms, and Kp < 3. Figure 8 shows the ionospheric parameters $h'F$ and h_mF_2 obtained on 29–30 June 2000. The dashed rectangle area shows the period when the structure passes over the zenith. Figure 9 shows the ionograms corresponding to this event.

[21] Events such as depicted in Figures 8 and 9 detected in our analysis were considered as manifestation of MSTIDs and the computed occurrence rate for the period from March 2000 to February 2001 (solar maximum) is shown in Figure 10.

4. Discussion

[22] In this work we have presented an extensive statistical study regarding on the solar cycle and seasonal dependence of the occurrence rate of MSTIDs in the low-latitude Brazilian sector. In this region we have observed a greater occurrence during solar minimum and winter time. Also, all observed cases are not related to geomagnetic storms. Features like the tendency of alignment from southwest to northeast, the direction of propagation (northwestward) and the tilt with the magnetic meridian (~20°) of
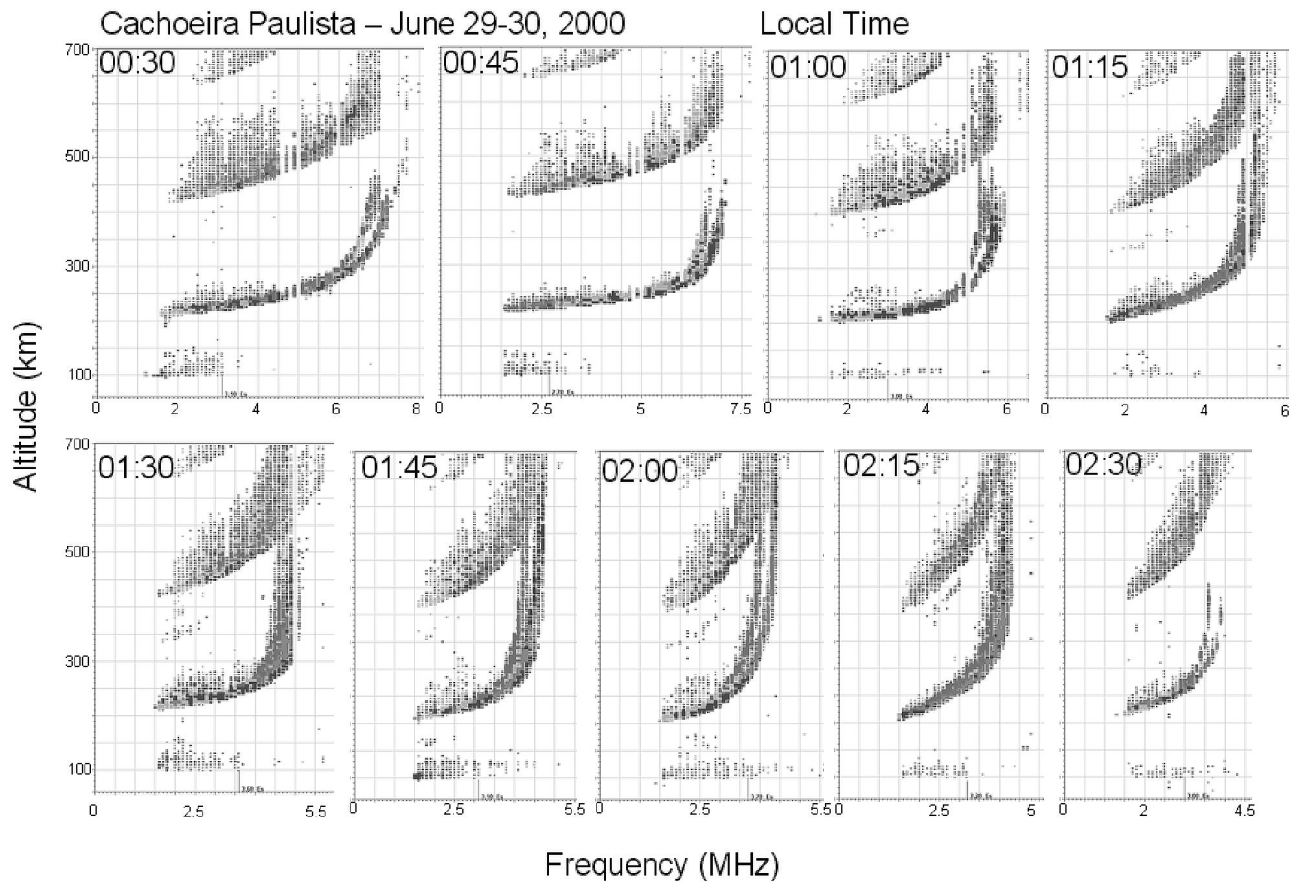
Figure 9. Ionograms showing the occurrence of spread F for the same time as the ionospheric parameters registering the rising of the F layer.

the dark bands led us to classify this phenomenon as being driven by midlatitude F region instabilities.

[23] The analysis made using all-sky images shows most MSTID occurrences during solar minimum, a minor percent-
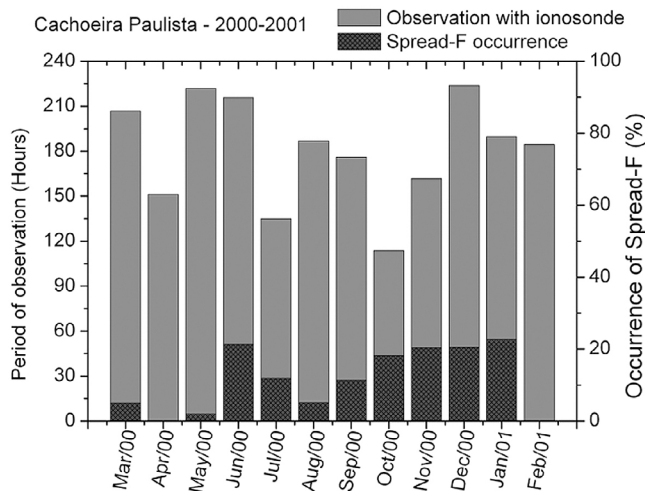

Figure 10. Statistical analysis of the occurrence of midlatitude spread F over Cachoeira Paulista during the period of solar maximum (2000–2001) based on F region ionograms.

age during descending and ascending solar activity periods, but no occurrences during solar maximum. One explanation to the inverse dependence with solar cycle is based on the Perkins instability theory [*Perkins*, 1973]. According to the Perkins theory, the growth rate of the instability is higher during solar minimum and lower during solar maximum, since it depends inversely to ion-neutral collision frequency.

[24] Regarding on the seasonality, we have observed a peak of occurrence during winter time. Since we have observed the occurrence of MSTIDs during geomagnetically quiet periods, it is possible that gravity waves from the low and medium atmosphere are acting like a seeding mechanism for the generation of the Perkins instability. Another possibility for explaining this feature can be based on the mapping electric fields between conjugated hemispheres. Observations made in geomagnetic conjugate points [*Otsuka et al.*, 2004] have showed mirrored structures in both hemispheres which suggest the important role of the polarization electric fields on the generation of MSTIDs.

[25] Ionospheric parameters $h'F$ and h_mF_2 shows sharp rises of the F layer during MSTID events. These rises are explained as being due to drifts $\mathbf{E_p}\mathbf{x}\mathbf{B}$, where $\mathbf{E_p}$ is the polarization electric field inside the MSTID structures. The electrodynamical coupling between the nighttime midlatitude ionospheric E_s and F region have been invoked as an explanation for the large polarization electric fields observed in the F region and the consequent uplifts of the F layer

which causes spread F [*Tsunoda and Cosgrove*, 2001]. *Haldoupis et al.* [2003] proposed a mechanism for spread F development in the midlatitude ionosphere driven by northward-upward electric fields, which are generated from a meridional polarization field inside an unstable E_s layer and maps to the F region via field lines. *Cosgrove and Tsunoda* [2004] derived a dispersion relation that describes the coupling behavior between E_s layer and Perkins instability. They showed that the coupled system is unstable and the electrodynamics interaction between instabilities acts to increase the growth rate of the global system.

[26] Finally, our analysis regarding the 1 year ionosonde data set for solar maximum have showed occurrence of MSTIDs during this phase of the solar cycle. The parameter $h'F$ in Figure 8 shows almost none variation and h_mF_2 shows almost 40 km displacement above 250 km height. During such events, the displacement of ionospheric layer is not sufficient to disturb the airglow layer and, consequently, dark band structures have not been registered in the all-sky images. Observations at midlatitudes are necessary to reinforce these statements and verify the mechanism of MSTID generation.

5. Summary

[27] In this study with all-sky images we have used a large data set, covering all phases of the solar cycle. On the basis of our observations regarding the MSTID propagation direction and its tilt to geomagnetic meridian around 20° westward, it seems that these dark bands were generated at medium latitudes, on the southern hemisphere, by the Perkins plasma instability process. Comparison between all-sky images and ionosonde data indicate that MSTIDs that propagate from southeast to northwest are able to produce spread F on ionograms. The main features of MSTIDs observed in the Brazilian low-latitude region can be summarized.

[28] 1. The main feature is their preferential alignment (southwest to northeast) and propagation direction (north-westward) at an altitude range of 220–350 km.

[29] 2. Most of the occurrences are during solar minimum conditions, followed by descending and ascending solar activity periods and no events were optically detected during solar maximum.

[30] 3. The seasonal occurrence rate shows a peak of occurrence during winter time in the low-latitude Brazilian sector.

[31] 4. All cases have been observed during geomagnetically quiet nights which suggest a coupling with the low atmosphere.

[32] 5. Analysis of ionosonde data shows sharp rises of the ionospheric F layer and close association with spread F.

[33] 6. Analysis regarding only ionosonde data during the solar maximum period (March 2000–February 2001) shows the occurrence of events with features similar of that observed during simultaneous analysis of both ionograms and all-sky images. Such events show rises not so sharp of F layer which are not able to diminish the O I 630 nm emission which can justify the lack of airglow signature.

References

Candido, C. M. N., A. A. Pimenta, J. A. Bittencourt, and F. Becker-Guedes (2008), Statistical analysis of the occurrence of medium-scale traveling ionospheric disturbances over Brazilian low latitudes using OI 630.0 nm emission all-sky images, *Geophys. Res. Lett.*, *35*, L17105, doi:10.1029/2008GL035043.

Cosgrove, R. B., and R. T. Tsunoda (2004), Instability of the E-F coupled nighttime midlatitude ionosphere, *J. Geophys. Res.*, *109*, A04305, doi:10.1029/2003JA010243.

Garcia, F. J., M. J. Taylor, and M. J. Kelley (1997), Two-dimensional spectral analysis of mesospheric airglow image data, *Appl. Opt.*, *36*, 7374–7385, doi:10.1364/AO.36.007374.

Garcia, F. J., M. C. Kelley, J. J. Makela, and C. S. Huang (2000), Airglow observations of mesoscale low-velocity traveling ionospheric disturbances at midlatitudes, *J. Geophys. Res.*, *105*, 18,407–18,415, doi:10.1029/1999JA000305.

Haldoupis, C., M. C. Kelley, G. C. Hussey, and S. Shalimov (2003), Role of unstable sporadic-E layers in the generation of midlatitude spread F, *J. Geophys. Res.*, *108*(A12), 1446, doi:10.1029/2003JA009956.

Martinis, C., J. Baumgardner, J. Wroten, and M. Mendillo (2010), Seasonal dependence of MSTIDs obtained from 630.0 nm airglow imaging at Arecibo, *Geophys. Res. Lett.*, *37*, L11103, doi:10.1029/2010GL043569.

Otsuka, Y., K. Shiokawa, T. Ogawa, and P. Wilkinson (2004), Geomagnetic conjugate observations of medium-scale traveling ionospheric disturbances at midlatitude using all-sky airglow imagers, *Geophys. Res. Lett.*, *31*, L15803, doi:10.1029/2004GL020262.

Perkins, F. (1973), Spread F and ionospheric currents, *J. Geophys. Res.*, *78*, 218–226, doi:10.1029/JA078i001p00218.

Pimenta, A. A., P. R. Fagundes, J. A. Bittencourt, and Y. Sahai (2001), Relevant aspects of equatorial plasma bubbles under different solar activity conditions, *Adv. Space Res.*, *27*, 1213–1218, doi:10.1016/S0273-1177(01)00200-9.

Pimenta, A. A., D. C. M. Amorim, and C. M. N. Candido (2008a), Thermospheric dark band structures at low latitudes in the Southern Hemisphere under different solar activity conditions: A study using OI 630 nm emission all-sky images, *Geophys. Res. Lett.*, *35*, L16103, doi:10.1029/2008GL034904.

Pimenta, A. A., M. C. Kelley, Y. Sahai, J. A. Bittencourt, and P. R. Fagundes (2008b), Thermospheric dark band structures observed in all-sky OI 630 nm emission images over the Brazilian low-latitude sector, *J. Geophys. Res.*, *113*, A01307, doi:10.1029/2007JA012444.

Reinisch, B. W., K. Bibl, D. F. Kitrosser, G. S. Sales, J. S. Tang, Z. M. Zhang, T. W. Bullett, and J. A. Ralls (1989), The Digisonde 256 ionospheric sounder, in *WITS Handbook: World Ionosphere/Thermosphere Study*, vol. 2, edited by C. H. Liu, pp. 350–382, Natl. Sci. Found., Urbana, Ill.

Shiokawa, K., C. Ihara, Y. Otsuka, and T. Ogawa (2003), Statistical study of nighttime medium-scale traveling ionospheric disturbances using midlatitude airglow images, *J. Geophys. Res.*, *108*(A1), 1052, doi:10.1029/2002JA009491.

Tsunoda, R. T., and R. B. Cosgrove (2001), Coupled electrodynamics in the nighttime midlatitude ionosphere, *Geophys. Res. Lett.*, *28*(22), 4171–4174, doi:10.1029/2001GL013245.

D. C. M. Amorim, J. A. Bittencourt, and A. A. Pimenta, Instituto Nacional de Pesquisas Espaciais, Sao Jose dos Campos 12227-010, Brazil. (danielle@laser.inpe.br)

P. R. Fagundes, Physics and Astronomy, Universidade do Vale do Paraiba, Sao Jose dos Campos 12244-000, Brazil.